Topics in Catalysis (2023) 66:973–984
https://doi.org/10.1007/s11244-022-01723-1

ORIGINAL PAPER

Selective Catalytic Reduction with Hydrogen for Exhaust gas after-treatment of Hydrogen Combustion Engines

Michael Borchers[1] · **Patrick Lott**[1] · **Olaf Deutschmann**[1,2]

Accepted: 10 October 2022 / Published online: 30 November 2022

Abstract
In this work, two palladium-based catalysts with either ZSM-5 or Zeolite Y as support material are tested for their performance in selective catalytic reduction of NOx with hydrogen (H_2-SCR). The ligh-toff measurements in synthetic exhaust gas mixtures typical for hydrogen combustion engines are supplemented by detailed catalyst characterization comprising N_2 physisorption, X-ray powder diffraction (XRD), hydrogen temperature programmed reduction (H_2-TPR) and ammonia temperature programmed desorption (NH_3-TPD). Introducing 10% or 20% TiO_2 into the catalyst formulations reduced the surface area and the number of acidic sites for both catalysts, however, more severely for the Zeolite Y-supported catalysts. The higher reducibility of the Pd particles that was uncovered by H_2-TPR resulted in an improved catalytic performance during the light-off measurements and substantially boosted NO conversion. Upon exposition to humid exhaust gas, the ZSM-5-supported catalysts showed a significant drop in performance, whereas the Zeolite Y-supported catalyst kept the high levels of conversion while shifting the selectivity from N_2O more toward NH_3 and N_2. The 1%Pd/20%TiO_2/HY catalyst subject to this work outperforms one of the most active and selective benchmark catalyst formulations, 1%Pd/5%V_2O_5/20%TiO_2-Al_2O_3, making Zeolite Y a promising support material for H_2-SCR catalyst formulations that allow efficient and selective NOx-removal from exhaust gases originating from hydrogen-fueled engines.

Keywords Hydrogen Internal Combustion Engine · Selective Catalytic Reduction with Hydrogen (H_2-SCR) · NOx Abatement · Palladium Catalyst · Zeolites

1 Introduction

Hydrogen-fueled internal combustion engines (H_2-ICEs) operated under lean conditions present a promising possibility for the total decarbonization of the transport sector in the upcoming years. Despite the advantage of net zero greenhouse gas emissions, significant amounts of thermal NOx generated by the reaction of oxygen and nitrogen during the combustion need to be treated. Apart from the well-established selective catalytic reduction (SCR) with ammonia originating from an urea water solution [1], also hydrogen can serve as reductant for converting NOx emissions at even lower exhaust gas temperatures *via* selective catalytic reduction (H_2-SCR). This would not only circumvent some inherent urea SCR problems like deposit formation [2] and ammonia slip [3], but would also make an additional tank for the SCR reductant redundant.

Noble metal catalysts with palladium and platinum as active species are the most promising for the H_2-SCR reaction [4], among which platinum shows an overall higher activity particularly at low temperatures, but generally at the cost of a lower selectivity compared to palladium catalysts [5–8]. However, a high selectivity toward nitrogen is of utmost importance as the main byproduct of the reaction is nitrous oxide (N_2O), which exhibits a 300 times higher greenhouse potential than carbon dioxide (CO_2) [9]. Depending on the exhaust gas composition, temperature and catalyst formulation, also ammonia (NH_3) and nitrogen dioxide (NO_2) are possible side products during the H_2-SCR process [10–12].

✉ Patrick Lott
patrick.lott@kit.edu

[1] Institute for Chemical Technology and Polymer Chemistry (ITCP), Karlsruhe Institute of Technology (KIT), Engesserstr. 20, 76131 Karlsruhe, Germany

[2] Institute for Catalysis Research and Technology (IKFT), Karlsruhe Institute of Technology (KIT), 76344 Eggenstein-Leopoldshafen, Germany

Modifications of the support material highly affect the catalytic performance of H_2-SCR catalysts, for instance, as described by Costa et al. who combined the high selectivity of a Pt/MgO catalyst with the high activity of a Pt/CeO_2 catalyst by preparing a Pt/Mg-Ce-O mixed-oxide catalyst exhibiting both advantages [6]. Another approach was employed by Qi and coworkers who added vanadium pentoxide to a $Pd/TiO_2/Al_2O_3$ catalyst, which eases the formation of active NH_4^+ intermediates on acidic V_2O_5 sites, hereby opening an additional pathway for NOx reduction and thus circumventing an activity drop around 200 °C that was observed when using a vanadia-free catalyst [13]. In this context, Li et al. were the first to systematically study the role of support acidity during H_2-SCR [14]. Their study points to a correlation between the catalyst's acidity and its NOx reduction activity as well as selectivity toward N_2, thus, zeolitic supports that intrinsically offer Brønsted acidic sites when doped with Al_2O_3 are highly attractive materials for H_2-SCR catalyst systems.

Since zeolite supports offer good thermal stability [15, 16], high tuneability and are commonly used in catalyst systems for NH_3-SCR [17], several groups suggested zeolitic and zeolite-related catalysts also in the field of H_2-SCR. By optimizing the preparation method, Wen achieved up to 70% NO conversion when using a Pd/MFI catalyst for H_2-SCR in a H_2O-free reaction gas mixture [18], while Zheng et al. could achieve NOx conversions of 99% with a ZSM-5-based Pt-catalyst [19]. In addition, TiO_2-promoted mesoporous materials were probed with platinum [20] and palladium [21] investigating the positive effect of TiO_2 on the reducibility of the noble metal particles and the enhancement in hydrogen spillover.

Despite these encouraging findings, the influence of these support materials on the H_2-SCR reaction and the complex interplay of NO, H_2 and exhaust compounds such as water (H_2O) remains unclear. Thus, the present study evaluates and examines zeolite-supported palladium catalysts for their applicability in H_2-SCR as a potential after-treatment for hydrogen combustion engine exhausts. A combination of catalytic activity measurements and detailed characterization aim at elucidating the support impact on both catalytic activity and product selectivity, hereby laying the foundation for further advancements in the field of H_2-SCR.

2 Experimental

2.1 Catalyst Preparation

The catalyst support materials ZSM-5 (Clariant, SM-27) and Zeolite Y (Zeolyst, CBV300) were calcined in air for 6 h at 500 °C and subsequently TiO_2 was precipitated from a $Ti(OBu)_4$ solution in ethanol for the Ti-containing catalysts. After drying for 1 h at 70 °C and calcination in air for 6 h at 500 °C, palladium was added *via* incipient wetness impregnation (IWI) using an aqueous tetraamminepalladium(II) nitrate solution (abcr, 5.0% Pd) followed by drying for 1 h at 70 °C and a calcination step at 500 °C for 6 h. Preparation of the $1\%Pd/5\%V_2O_5/20\%TiO_2$-$Al_2O_3$ catalyst, which was already subject of previous studies [11, 13] and which served as a benchmark catalyst for the current work, is described in an earlier publication [11]. In addition, a baseline Pd/Al_2O_3 reference system was prepared by IWI of γ-Al_2O_3, analogous to the procedure described above.

2.2 Catalyst Characterization

N_2-physisorption measurements of the catalyst powders were performed using a BELSORP-mini II instrument (BEL Japan) after degassing for 2 h at 300 °C. The surface area and total pore volume were then obtained via the method of Brunauer, Emmett and Teller (BET) [22].

For X-ray diffraction (XRD) measurements, an X'PERT PRO diffractometer (PANalytical) was employed using Cu K_α radiation (wavelength of 0.154 nm) and scanning 2θ from 20 to 80° with a step size of 0.017° and an acquisition time of 0.44 s.

Inductively coupled plasma optical emission spectroscopy (ICP-OES) was used to validate the elemental composition of the different powder catalysts.

Temperature-programmed reduction with hydrogen (H_2-TPR) was conducted at an AutoChem II unit (micromeritics). After an oxidative pretreatment (10% O_2 in He, 10 K min^{-1} to 500 °C), the H_2-TPR was measured with 50 mL min^{-1} of 10% H_2 in Ar from − 50 to 600 °C with 10 K min^{-1} using a cryogenic cooler with liquid N_2. The effluent gas stream was analyzed by means of a thermal conductivity detector (TCD).

Temperature-programmed desorption of ammonia (NH_3-TPD) experiments were performed in a synthetic gas testing bench that was controlled by an in-house developed LabVIEW-based software tool. While mass flow controllers (MFC) from Bronkhorst were used to create the well-defined (reaction) gas mixture from pure gases, water was added via a combination of a controlled evaporator mixer (CEM, Bronkhorst) with a liquid flow controller (LiquiFlow, Bronkhorst). 300 mg of sample and 700 mg of quartz sand in a size distribution of 125–250 µm were mixed and fixed with quartz glass wool inside a quartz glass tubular reactor (inner diameter: 8 mm) embedded in an electric furnace. Two thermocouples (type N) up- and downstream of the catalyst bed ensured a sufficient temperature control. After passing through the reactor, the gas is then analyzed by an FT-IR spectrometer (MultiGas 2030, MKS Instruments).

Table 1 Gas mixtures and GHSV used in the catalytic activity tests

Gas mixture	NO [vppm]	H_2 [vppm]	O_2 [%]	H_2O [%]	N_2	GHSV [h^{-1}]
Dry mixture	1000	5000	10	0	balance	60,000
Wet mixture	1000	5000	10	10	balance	60,000

Table 2 Characterization results of N_2-physisorption and elemental analysis by ICP-OES

Target catalyst formulation	BET Surface area [$m^2\ g^{-1}$]	Total pore volume [$cm^3\ g^{-1}$]	Al_2O_3 [wt.-%]	SiO_2 [wt.-%]	TiO_2 [wt.-%]	Pd [wt.-%]
1%Pd/ZSM-5	386	0.201	6.3	92.9	0.0	0.84
1%Pd/10%TiO_2/ZSM-5	352	0.204	5.5	82.7	10.8	0.92
1%Pd/20%TiO_2/ZSM-5	318	0.194	4.8	72.7	21.6	0.91
1%Pd/HY	510	0.234	24.3	74.7	0.0	0.99
1%Pd/10%TiO_2/HY	304	0.164	21.6	65.9	11.4	1.04
1%Pd/20%TiO_2/HY	264	0.162	19.9	55.2	23.6	1.25

During the course of an NH_3-TPD experiment, 1 slpm containing 500 ppm NH_3, 10% O_2 and 10% H_2O in N_2 was used to saturate the catalyst at 200 °C for 45 min. Subsequently, the NH_3-MFC was closed to purge the catalyst for 20 min before starting the desorption step consisting of heating to 500 °C at 10 K min^{-1} in 10% O_2 and 10% H_2O in N_2. Integrating the NH_3-signal from the FT-IR over the time yields the amount of stored ammonia per sample weight.

2.3 Catalytic Test Procedure

The catalytic activity tests were conducted in the same setup that was employed for the NH_3-TPD tests; reactor dimensions, powder catalyst sample size and dilution were also kept consistent. Note that the powder catalyst grain size of 125–250 µm minimizes external mass transfer limitations [23], hence, the origin of kinetic phenomena observed during the catalytic tests is exclusively related to temperature and catalytic effects. As illustrated in Fig. S1, the testing procedure started with a degreening of the fresh catalyst powder for 1 h at 500 °C under wet reaction conditions (Table 1), followed by an oxidation step (10% O_2 in N_2) for 20 min at 500 °C. The reactor was then cooled to 100 °C and three successive light-off-light-out-cycles from 100 to 300 °C with 2 K min^{-1} were conducted in dry reaction gas (Table 1). After a second oxidation step of 10% O_2 in N_2 for 20 min at 500 °C, these three cycles were then repeated under wet reaction conditions (+ 10% H_2O, Table 1). The gas flow was balanced with N_2 to keep a flow rate of 1 slpm and thus a gas hourly space velocity (GHSV) of 60 000 h^{-1}. As the effluent gas concentrations are also analyzed by FT-IR spectroscopy, the IR-inactive species N_2 is calculated *via* the N-containing species balance and H_2 conversion is calculated from the produced H_2O and NH_3. The selectivities were calculated using the following equations. The inlet flows were measured *via* a bypass line feeding directly into the analytics without passing the reactor and thus the catalyst:

$$S\left(\mathrm{N_2O}\right) = \frac{2 \cdot \left(\dot{n}_{\mathrm{N_2O,out}} - \dot{n}_{\mathrm{N_2O,in}}\right)}{\dot{n}_{\mathrm{NO,in}} - \dot{n}_{\mathrm{NO,out}}} \quad (1)$$

$$S\left(\mathrm{NO_2}\right) = \frac{\dot{n}_{\mathrm{NO_2,out}} - \dot{n}_{\mathrm{NO_2,in}}}{\dot{n}_{\mathrm{NO,in}} - \dot{n}_{\mathrm{NO,out}}} \quad (2)$$

$$S\left(\mathrm{NH_3}\right) = \frac{\dot{n}_{\mathrm{NH_3,out}}}{\dot{n}_{\mathrm{NO,in}} - \dot{n}_{\mathrm{NO,out}}} \quad (3)$$

$$S\left(\mathrm{N_2}\right) = 1 - S\left(\mathrm{N_2O}\right) - S\left(\mathrm{NO_2}\right) - S\left(\mathrm{NH_3}\right) \quad (4)$$

3 Results and Discussion

3.1 Catalyst Characterization

The N_2-physisorption results (Table 2) clearly indicate different effects of the titania precipitation on the zeolitic materials. While the ZSM-5-based catalysts show only a small decrease in surface area (9% and 18% loss with 10% and 20% TiO_2, respectively), the surface area of the HY-based catalysts nearly drops in half (40% and 48% loss with 10% and 20% TiO_2, respectively). Moreover, the difference between 10% and 20% of TiO_2 is less prominent in the HY-supported catalysts than it is for the ZSM-5-based ones. These findings can be explained in the light of the XRD-results (Fig. S2). For the Pd/zeolite catalysts without titania, we observed only the diffraction patterns of the pure zeolites in both cases, which suggests a high dispersion of Pd for these catalysts. Once TiO_2 is added, the X-ray diffraction patterns suggest a coexistence of zeolite and antatase-TiO_2 [24] for the ZSM-5-supported catalysts, whereas the HY-supported materials gradually lose their typical zeolitic reflexes upon TiO_2 precipitation. Regarding the physisorption results, we can assume that TiO_2 preferentially forms a partially pore-blocking layer on the outer surface of Zeolite Y that results in a higher surface area loss than for the

Table 3 Peak locations in the H_2-TPR experiments for the examined catalysts and adsorbed amount of NH_3 and total N-species of the catalysts during the NH_3-TPD experiments

Target Catalyst formulation	PdO reduction temperature [°C]	2nd reduction peak [°C]	Ads. NH_3 [mmol g^{-1}]	Total ads. N-species [mmol g^{-1}]
1%Pd/ZSM-5	16	--	0.394	0.394
1%Pd/10%TiO_2/ZSM-5	15	--	0.277	0.277
1%Pd/20%TiO_2/ZSM-5	11	--	0.269	0.269
1%Pd/HY	38	80	0.128	0.351
1%Pd/10%TiO_2/HY	16	76	0.166	0.181
1%Pd/20%TiO_2/HY	18	73	0.060	0.072
1%Pd/Al_2O_3	43	--	0.011	0.011
1%Pd/5%V_2O_5/20%TiO_2/Al_2O_3	8	81	0.017	0.017

Total ads. N-species = adsorbed $NH_3 + NO + 2\ N_2O$

ZSM-5-based catalysts that may exhibit TiO_2 islands on the zeolite surface.

Regarding the H_2-TPR profiles, Table 3 summarizes the relevant peak locations for each catalyst system. The 1%Pd/ZSM-5 catalyst (Fig. S3a) exhibits one sharp peak at 16 °C followed by a small negative peak at around 45 °C. The sharp peak can be attributed to the reduction of PdO while the negative peak indicates the decomposition of a palladium hydride species, which is formed from reduced Pd^0 species at lower temperatures [12]. The incline at the start of the measurement is also observable with the reduced catalyst and can be explained by the adsorption of argon from the 10%H_2/Ar feed gas in the zeolite pores causing a signal at the thermal conductivity detector [25]. The addition of titania to the ZSM-5-supported catalyst subsequently shifts the PdO reduction peak toward 15 °C and 11 °C for 10% and 20% TiO_2, respectively, and further sharpens the peak. Therefore, it can be concluded that TiO_2 is able to stabilize the Pd particles in their reduced form, which is considered more active for the H_2-SCR reaction than PdO [11, 26, 27]. Unlike the ZSM-5-supported catalysts, the 1%Pd/HY catalyst (Fig. S3b) exhibits two reduction peaks at 38 and 80 °C, which are attributed to the reduction of PdO and dispersed Pd^{2+} [25, 28], respectively, in addition to the Ar adsorption peak. When either 10% or 20% TiO_2 are added to the HY-based formulation, these reduction peaks shift toward lower temperatures, namely to 16 and 18 °C for PdO reduction and to 76 °C and 73 °C for the Pd^{2+} reduction peak, respectively. In addition, an increased TiO_2 loading rises the intensity of the Pd^{2+} peak, indicating a subsequent migration of Pd into the zeolitic system with higher TiO_2 loading. For the 1%Pd/5%V_2O_5/20%TiO_2-Al_2O_3 benchmark catalyst a sharp PdO reduction peak is found at 8 °C (Fig. S4) accompanied by the V_2O_5 reduction peak around 80 °C already shown in our previous work on this catalyst [11]. On the contrary, for Pd/Al_2O_3, only a single small, broad peak at 43 °C can be observed, most likely originating from PdO reduction.

Since the number of Brønsted acidic sites directly correlates to the amount of adsorbed NH_3, the NH_3-TPD measurements (Table 3, Figs. S5-S8) provide direct information on the catalyst's acidity that is considered a key parameter governing the catalytic activity [14]. Although the adsorption of NH_3 on palladium can also occur [29], the contribution to the overall NH_3 adsorption is assumed to be negligibly low in the studied formulations due to a much higher abundance of Brønsted acid sites. With only 0.011 and 0.017 mmol g^{-1}, respectively, 1%Pd/Al_2O_3 and 1%Pd/5%V_2O_5/20%TiO_2-Al_2O_3 store substantially less ammonia than the zeolite-based materials and the vanadia promotor has only a minor positive effect. Furthermore, the NH_3-TPD measurements with ZSM-5-supported catalysts showed that the addition of TiO_2 reduces the number of acidic sites by approximately 30%, with only minor differences between the catalyst samples containing either 10% or 20% of TiO_2. Unlike the aforementioned catalysts, the 1%Pd/HY catalyst shows two additional features during the NH_3-TPD measurements. On the one hand, high levels of NO and N_2O are formed during the desorption step of the previously saturated and purged sample. Presumably, those are reaction products originating from ammonia oxidation over the highly dispersed Pd^{2+} species whose existence on the HY-based samples was uncovered by H_2-TPR and which are known to exhibit higher activity toward NH_3 oxidation than PdO particles [30, 31]. To take this into account, those signals were also integrated and added to the NH_3 signal for a more thorough comparison. On the other hand, the HY-supported catalysts exhibit a decreasing NH_3 storage capacity with subsequent adsorption-desorption cycles (data not shown), possibly due to temperature-induced or chemically induced morphological changes. Since material changes and aging phenomena are beyond the scope of the present study and will be subject of a follow-up publication, only the first cycle is discussed in this work. While the total amount of adsorbed nitrogen-containing species is in the same range for Pd/HY and Pd/ZSM-5, the introduction of TiO_2 showed a much more severe effect on the HY-supported catalyst. The addition of 10% and 20% of TiO_2, respectively, reduced the ammonia storage capacity of the HY-based samples by 48% and 79% which coincides well with the large loss in surface area that was observed in the N_2-physisorption data.

Hence, a blockage of acidic surface sites along with a reduction of the physically available surface due to titania deposition can be assumed.

3.2 Catalyst Activity Tests

As described above, light-off measurements in a synthetic gas test bench allowed to probe the catalytic activity for the H_2-SCR reaction over the different powder catalysts investigated in this work. When discussing the results obtained, particular focus is laid not only on the NOx conversion, but also on the selectivity to N_2 along with the evolution of undesired byproducts. Although in the dry gas mixture (1000 ppm NO, 5000 ppm H_2, 10% O_2 in N_2; Fig. 1) 1%Pd/ZSM-5 and 1%Pd/HY readily convert H_2 and a temperature of 50% conversion (T_{50}) of 134 °C is found over Pd/ZSM-5 and a T_{50} of 171 °C is observed over the HY-supported catalyst, the NO conversion does not exceed 23%. While both catalysts exhibit a similar N_2O selectivity, Pd/HY is substantially less active for NO oxidation to NO_2 than Pd/ZSM-5; notably, ammonia formation is negligible over both catalyst formulations. Comparing the two Pd-zeolite catalysts to the 1%Pd/Al_2O_3 reference catalyst (Fig. S15) indicates no immediate, substantial advantage of the zeolitic support itself over the conventional γ-Al_2O_3-support material, as the overall NO conversion is in the same range for all three catalysts. Only the higher selectivity to N_2 observed with the Pd/HY catalyst constitutes a minor benefit.

For both catalyst systems, the addition of 10% TiO_2 significantly promotes the NO conversion (Fig. 2): The maximum NO conversion increases to 80% for 1%Pd/10%TiO_2/ZSM-5 and 85% for 1%Pd/10%TiO_2/HY. In addition, a local NO conversion maximum around 150 °C is found for both samples, which is common for Pd-containing H_2-SCR catalysts [13, 32, 33]. Furthermore, the TiO_2 addition decreases the selectivity to NO_2 while benefiting N_2O and NH_3 formation, which is essentially a shift from oxidized toward reduced products of NO. This indicates a change in the reaction mechanism already observed for other reducible support materials in the context of H_2-SCR, whereby adsorbed NOx-species as well as hydrogen atoms undergo spill-over from the noble metal to the support, with the actual reduction of NOx by hydrogen atoms taking place at the noble metal-support interface [34]. The same selectivity changes are observed for the HY-based catalyst, however, more pronounced; i.e. a maximum NH_3 selectivity of 25% is reached around 230 °C, which in consequence decreases the N_2 selectivity to 47%. Regarding the hydrogen conversion, the 1%Pd/10%TiO_2/HY catalyst shows a steeper incline and an overall shift of T_{50} by 19 °C toward lower temperature than its unpromoted counterpart, which goes along with an earlier onset of NO conversion. As indicated by the lower reduction temperature in the TPR results, this shift might be explained by the higher reducibility of Pd-sites that is induced by the presence of TiO_2. Since the oxidation of hydrogen presumably involves a surface layer of PdO and weakly adsorbed H_2 [35], we can assume a facilitated hydrogen activation over catalysts exhibiting a higher reducibility [26]. Since from a mechanistic point of view the dissociative adsorption of NO is followed by reaction of N atoms with H atoms to form NH_3 and eventually NH_4^+-species that react with NO to N_2, an earlier H_2 activation also benefits the SCR of NO. The evolution of NH_3 that was particularly observed between 190 and 300 °C for 1%Pd/10%TiO_2/HY and to lower extent between 225 and 275 °C also over 1%Pd/10%TiO_2/ZSM-5 supports this hypothesis.

A further increase of the TiO_2 content from 10 to 20% (Fig. 3) leads to a small shift of the hydrogen light-off toward lower temperature of 11 °C for the ZSM-5- and 6 °C for the HY-supported catalyst. While compared to the samples with 10% TiO_2 the overall NO conversion stays in a similar range for samples with 20% TiO_2 content, the deNOx activity in the medium-temperature range between 175 and 275 °C slightly decreases, whereas it rises in the low-temperature regime between 100 and 175 °C. As indicated by the decrease in ammonia uptake during the NH_3-TPD experiments (Table 3), the higher TiO_2 loading causes a blockage of acidic sites, which are considered a prerequisite for high activity in this medium temperature range [13]. Hence, their loss may explain the small activity decline between 175 and 275 °C. In contrast, the small rise of NOx conversion between 100 and 175 °C may be due to the promotion of a different reaction pathway that was suggested by Hong et al. [36] for the low-temperature regime. Herein, H_2 dissociatively adsorbs on the noble metal, is transferred to the support and reacts with adsorbed NOx species. Since the acidity drops with increasing titania content, the support's tendency towards NOx and H adsorption changes, which can directly impact the reaction mechanism and hereby change the dominant reaction pathway. Overall, the most interesting finding is the change in selectivity: Neither NH_3 nor NO_2 are formed in considerable amounts over 1%Pd/20%TiO_2/ZSM-5 (Fig. 3a). Similarly, the increase of TiO_2 loading substantially reduced NH_3 formation over the HY-supported catalyst, and only minor amounts of NO_2 evolve (Fig. 3b). Presumably, the blockage of acidic sites on the zeolites with increasing titania content reduces the formation of NH_x-intermediates that could turn into effluent NH_3. Albeit this results in an overall higher N_2 selectivity for the 1%Pd/20%TiO_2/HY catalyst compared to the 10%TiO_2 counterpart, the N_2O selectivity reaches a maximum of almost 40% around 250 °C.

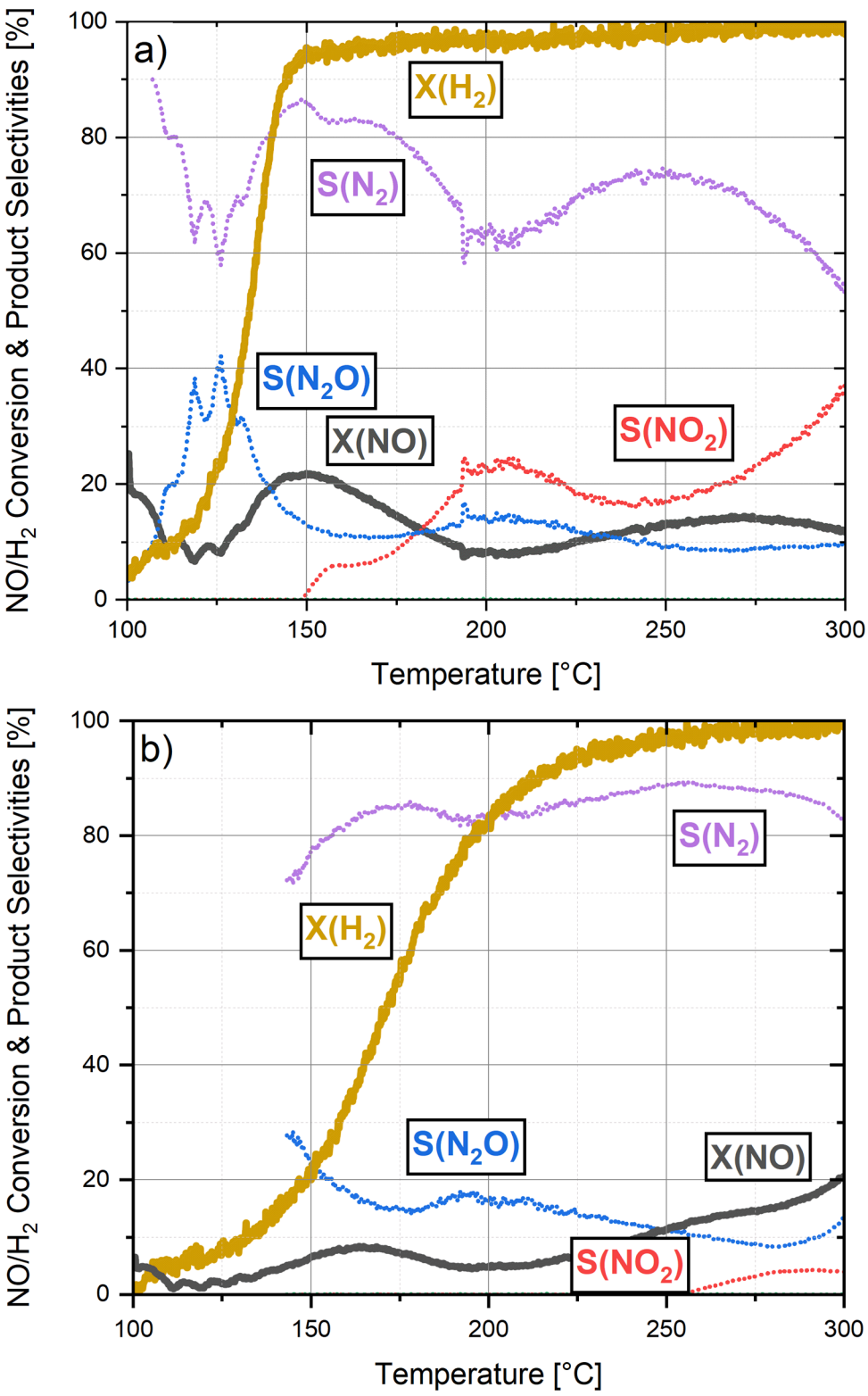

Fig. 1 Light-off curves of 1%Pd/ZSM-5 (a) and 1%Pd/HY (b) in the dry gas mixture (cf. Table 1). NO (grey) and H_2 (brown) conversions are shown as solid lines and N_2 (purple), N_2O (blue), NO_2 (red) and NH_3 (green) selectivities as dotted lines

Throughout these activity tests, an increased N_2O selectivity was observed at low temperature (100–175 °C) after introducing TiO_2 to the given compositions. Without further mechanistic studies we can only speculate on the reason for this effect, which might be partly related to the adsorption-desorption mechanism proposed in literature [4]. Therein, NO is adsorbed on the catalytic surface as NO_{ad} and can then dissociate into N_{ad} and O_{ad} species able to form N_2

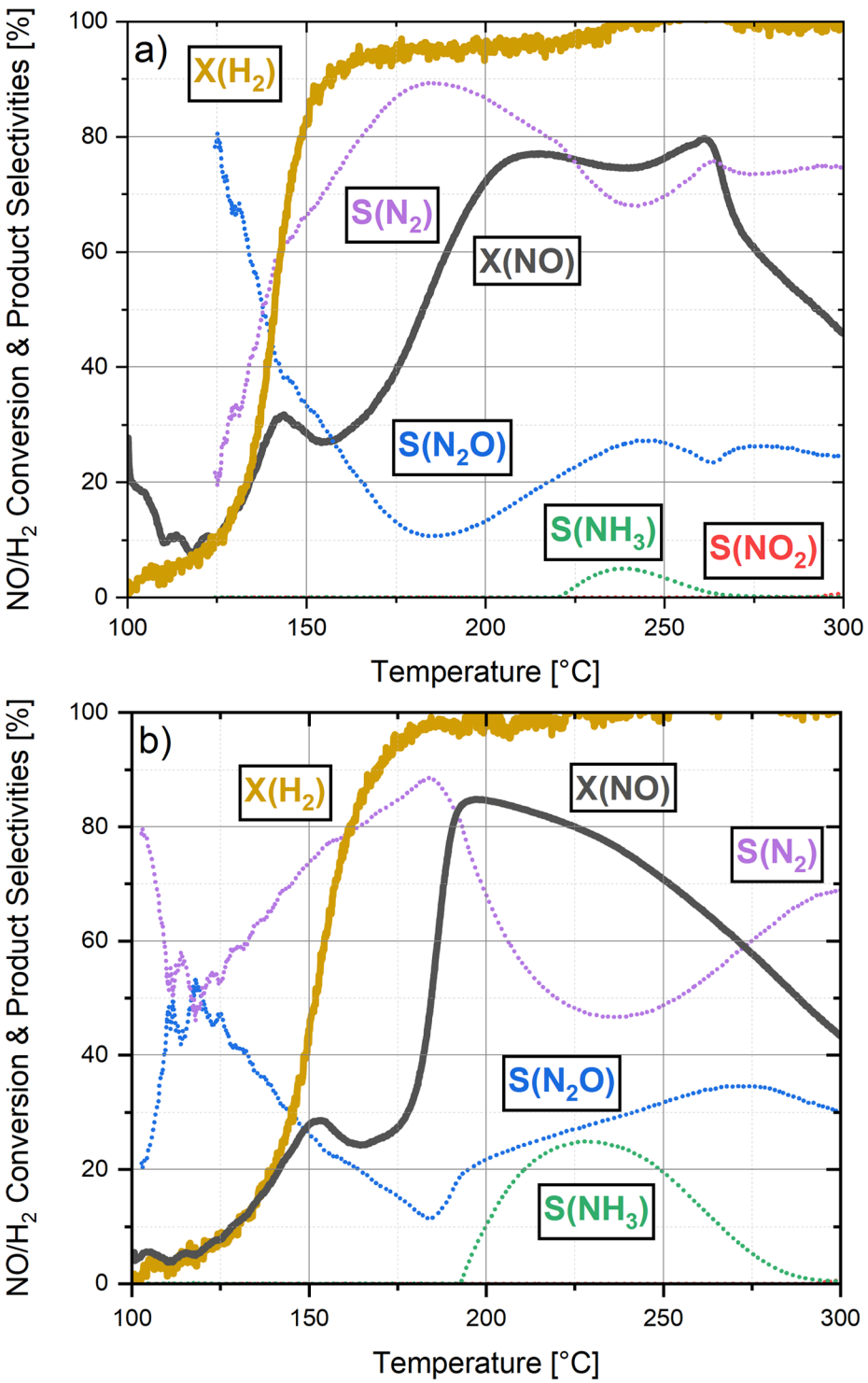

Fig. 2 Light-off curves of 1%Pd/10%TiO_2/ZSM-5 (a) and 1%Pd/10%TiO_2/HY (b) in the dry gas mixture (cf. Table 1). NO (grey) and H_2 (brown) conversions are shown as solid lines and N_2 (purple), N_2O (blue), NO_2 (red) and NH_3 (green) selectivities as dotted lines

from two N_{ad} or N_2O from NO_{ad} and N_{ad}. Combining this mechanism with our observed increase in N_2O formation, we can assume a higher NO_{ad} to N_{ad} ratio on the surface with TiO_2 promotion at low temperature. This shift can be explained by TiO_2 stabilizing Pd in its reduced state and thus enhancing NO adsorption on active sites already at lower temperatures where the bond cleavage kinetics to form N_{ad} and O_{ad} are still low.

So far, the catalytic activity has only been discussed in a model-like dry reaction gas mixture. However, hydrogen combustion engines emit considerable amounts of steam [37] that can influence both activity and selectivity of noble

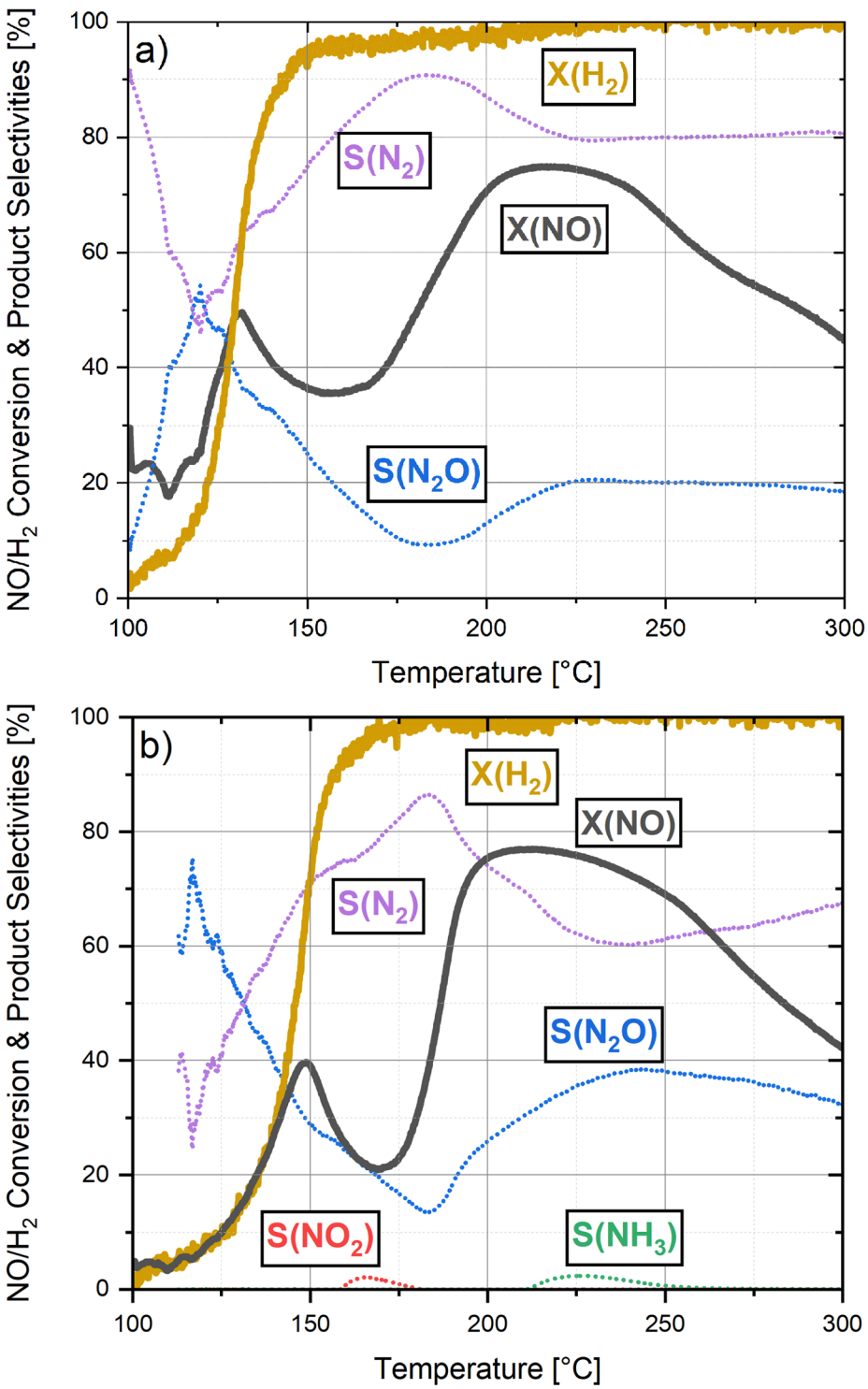

Fig. 3 Light-off curves of 1%Pd/20%TiO_2/ZSM-5 (a) and 1%Pd/20%TiO_2/HY (b) in the dry gas mixture (cf. Table 1). NO (grey) and H_2 (brown) conversions are shown as solid lines and N_2 (purple), N_2O (blue), NO_2 (red) and NH_3 (green) selectivities as dotted lines

metal based H_2-SCR catalysts, since H_2O can strongly adsorb on the active sites [38, 39]. Adding 10% H_2O to the feed gas mix (wet gas mixture, Table 1) during the light-off tests with the catalysts containing 20%TiO_2-promotor (Fig. 4) had a severe effect on the ZSM-5-supported catalyst. Compared to the dry conditions, the NO conversion over 1%Pd/20%TiO_2/ZSM-5 decreased strongly in the medium-temperature regime and even undercuts 10% conversion between 180 and 210 °C. This significant activity drop is also observed for the TiO_2-free and 10%TiO_2 ZSM-5 sample (Figs. S9, S10) and renders these systems inappropriate for exhaust gas aftertreatment systems with highly humid

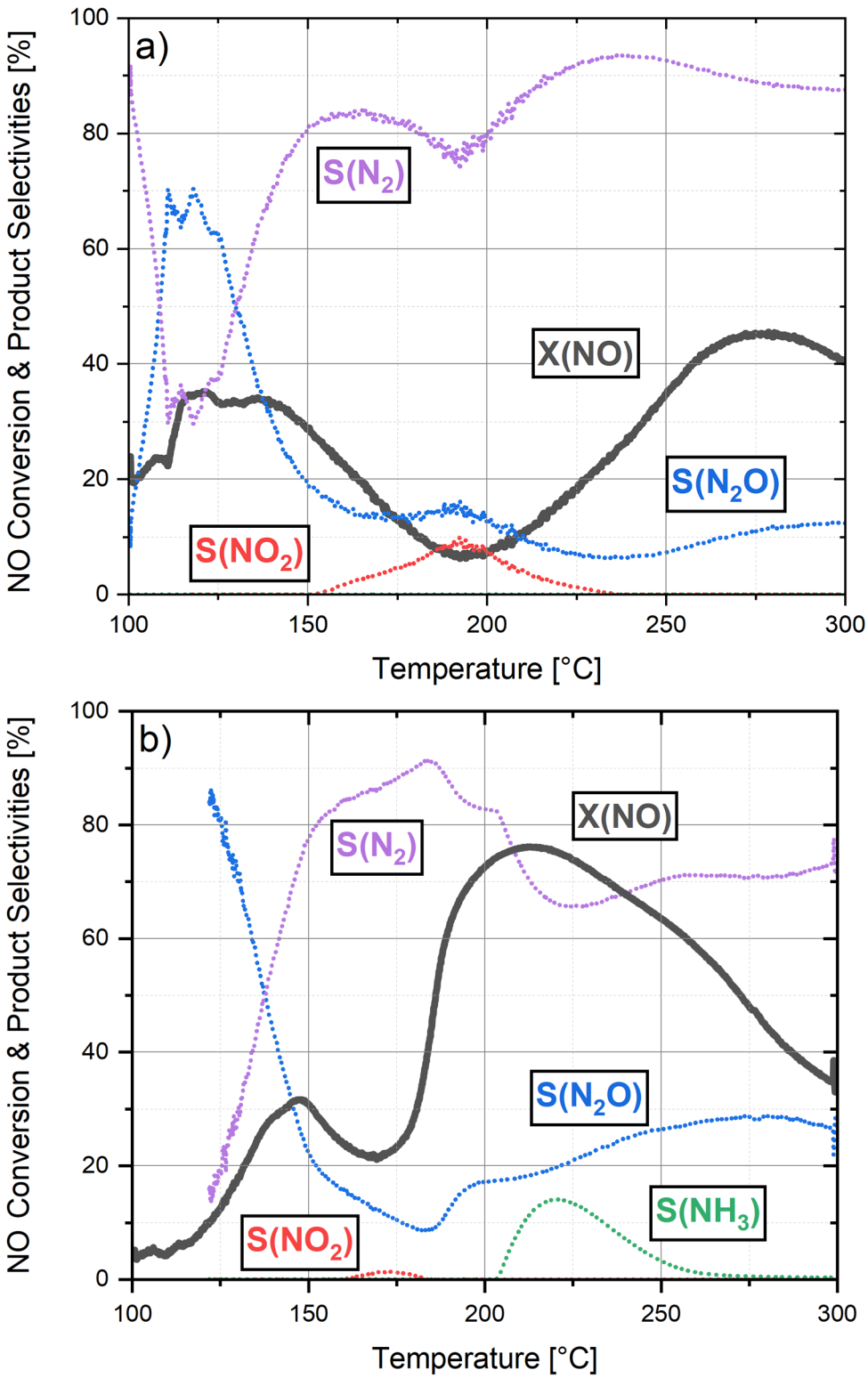

Fig. 4 Light-off curves of 1%Pd/20%TiO_2/ZSM-5 (a) and 1%Pd/20%TiO_2/HY (b) in the wet gas mixture (cf. Table 1). NO (grey) conversion is shown as a solid line and N_2 (purple), N_2O (blue), NO_2 (red) and NH_3 (green) selectivities as dotted lines

exhaust. In this regard, our findings support earlier results by Zhao et al., who observed an inhibited H_2-SCR reaction over Pt/ZSM-5 that was caused by competitive adsorption of NOx and water on the active sites [39]. Especially in the temperature regime between 150 and 250 °C, where the reaction is predominantly controlled by NO adsorption, we assume a similar behavior for our palladium-based catalysts supported on ZSM-5.

In contrast, 1%Pd/20%TiO_2/HY exhibits comparably good water tolerance: The NO conversion is only slightly

inhibited in the presence of steam and the addition of water even led to a decrease in N_2O formation. Despite a moderate increase in NH_3 selectivity, the lower N_2O levels particularly benefit the N_2 selectivity. A possible explanation for the lower effect of water on the activity of the HY-supported catalysts can be the occurrence of another reaction mechanism happening on the dispersed Pd^{2+} species. These Pd^{2+} species are known to be vital for NO activation in the related CH_4-SCR [40–42] and among the samples tested during this study, the H_2-TPR data suggest Pd^{2+} species only for the HY-supported catalysts. This indicates either a very low amount of Pd^{2+} species on the ZSM-5-supported catalysts that is beyond the detection limit of our analytics (AutoChem II unit, micromeritics, equipped with a TCD) or a complete lack of such species within the ZSM-5 framework. However, as reported by several groups, Pd^{2+} can also exist in ZSM-5 structures [42, 43]. The reason for the higher tendency of our HY-supported catalysts to form dispersed Pd^{2+} species compared to the ZSM-5-supported catalysts might be the differences in pore diameter (0.5 nm for ZSM-5 and 0.7-0.8 nm for Zeolite Y [44]) and aluminum content (Table 2) of the two zeolites. A higher abundance of negatively charged AlO_2^- units is supposed to facilitate the stabilization of Pd^{2+} species within the zeolite structure and the higher pore diameter of HY allows a better accessibility to the porous framework of the support, where Pd^{2+} is typically located on zeolites [45]. While the introduction of water severely inhibits the NO adsorption at the aggregated Pd sites, most likely in the oxidized PdO state, the Pd^{2+}-sites might still be able to convert NO and thereby keep the overall activity of the HY-based catalysts at a high level. Furthermore, this shift between two reaction mechanisms would be able to explain the changes in selectivity for the HY-catalyst in the mentioned temperature regime. Beyond the findings reported herein, more detailed investigations on such phenomena are highly desirable in the future, since involving oxidation-state sensitive and surface adsorbate sensitive techniques will add new facets to the fundamental understanding at an atomic scale.

Compared to a $1\%Pd/5\%V_2O_5/20\%TiO_2/Al_2O_3$ benchmark catalyst that was subject of an earlier study of our group [11] and that was also tested as a powder catalyst in dry and wet feed for the current study (Figs. S13, S14), the $1\%Pd/20\%TiO_2$/HY system exhibits a major improvement with regard to NO conversion and overall N_2 selectivity, particularly in the presence of water. We assume that the increased activity and selectivity of the HY-supported catalyst is related to two material properties: the higher surface area (264 $m^2\ g^{-1}$ versus 158 $m^2\ g^{-1}$ [11]) as determined by N_2-physisorption and the much higher number of acidic sites that was revealed by the NH_3-TPD experiments (Table 3). Assuming that the NO reduction predominantly proceeds *via* an NH_4^+-based reaction mechanism that was previously claimed for Pd- and Pt-based catalysts [13, 46, 47], the increased number of Brønsted acid sites on the catalyst presumably eases NH_4^+-formation by reaction of surface-adsorbed N and H atoms that originate from (dissociative) NO and H_2 adsorption on the noble metal and subsequent spillover to the support. These NH_4^+-species can then react with NOx species to form N_2 (and H_2O). Since the noble metal – support interface was identified as particularly important, allowing a bifunctional mechanism with adsorption/desorption reactions on the noble metal and spillover of surface species to and from the reducible support [47, 48], the high surface area of the HY-based sample offers more available surface sites than the Al_2O_3-supported benchmark catalyst.

4 Conclusion

Our study shows the potential of zeolite frameworks as support materials for selective catalytic reduction of NO with hydrogen under conditions typical for exhausts of hydrogen internal combustion engines. Although the activity of Pd/ZSM-5 and Pd/HY for H_2-SCR was comparably low, the precipitation of TiO_2 onto the zeolite drastically increased the NO conversion. Even though the addition of 10% and 20% of TiO_2 decreased the catalysts' surface area and the number of acidic sites, the promotional effect regarding the H_2-SCR clearly outweighs the negative impacts. In addition to a small activity shift toward lower temperature, which presumably originates from further blockage of acidic sites by the precipitated TiO_2, the difference in TiO_2 loading mainly affected the selectivity of the catalysts. Irrespective of the zeolitic material used as support, the samples containing 20% TiO_2 formed less ammonia thereby exhibit an increased selectivity toward N_2 compared to their counterparts containing 10% TiO_2.

In contrast, the catalyst's tolerance toward the inevitable exhaust component water strongly depends on the zeolite used as support. In a humid reaction gas mixture that is representative for H_2 combustion engine off-gases, the ZSM-5-based catalysts showed a severe NO conversion decline in the temperature range of 175 to 275 °C, whereas NO conversion over the HY-based catalysts was only insignificantly affected and the product selectivity slightly shifted from N_2O toward N_2 and NH_3. This difference might be explained by the presence of dispersed Pd^{2+} species on the HY-supported catalysts, which could not be observed in the H_2-TPR experiments for our ZSM-5-based samples. With regard to activity and selectivity, the $1\%Pd/20\%TiO_2$/HY catalyst presented in this work outperforms a previously investigated benchmark catalyst, namely $1\%Pd/5\%V_2O_5/20\%TiO_2/Al_2O_3$

[11], which underscores the high potential of zeolitic material utilization in the field of H_2-SCR. Last but not least, the extraction of kinetic parameters from our present results allows to develop and calibrate a micro-kinetic model for a Pd-based benchmark H_2-SCR system, which represents the first step towards comprehensive simulations of an overall exhaust gas after-treatment system for modern hydrogen combustion engines.

Supplementary Information The online version contains supplementary material available at https://doi.org/10.1007/s11244-022-01723-1.

Acknowledgements This work was financially supported by the Helmholtz-Program MTET: Materials and Technologies for the Energy Transition. The authors want to acknowledge F. Jerry for his contribution during his master's thesis, M. Makowiak for the N_2-physisorption measurements, D. Neukum for the XRD measurements and Dr. T. Bergfeldt (IAM, KIT) for the ICP-OES-measurements.

Funding Open Access funding enabled and organized by Projekt DEAL.

References

1. Damma D, Ettireddy P, Reddy B, Smirniotis P (2019) A Review of Low Temperature NH_3-SCR for Removal of NOx. Catalysts 9:349. https://doi.org/10.3390/catal9040349
2. Tischer S, Börnhorst M, Amsler J, Schoch G, Deutschmann O (2019) Thermodynamics and reaction mechanism of urea decomposition. Phys Chem Chem Phys 21:16785–16797. https://doi.org/10.1039/c9cp01529a
3. Colombo M, Nova I, Tronconi E (2012) A simplified approach to modeling of dual-layer ammonia slip catalysts. Chem Eng Sci 75:75–83. https://doi.org/10.1016/j.ces.2012.02.044
4. Hu Z, Yang RT (2019) 110th Anniversary: Recent Progress and Future Challenges in Selective Catalytic Reduction of NO by H_2 in the Presence of O_2. Ind Eng Chem Res 58:10140–10153. https://doi.org/10.1021/acs.iecr.9b01843
5. Eßer E, Schröder D, Nartova AV, Dmitrachkov AM, Kureti S (2022) Reduction of NOx by H_2 on WO_x-Promoted $Pt/Al_2O_3/SiO_2$ Catalysts Under O_2-Rich Conditions. Catal Lett 152:1598–1610. https://doi.org/10.1007/s10562-021-03747-w
6. Costa CN, Efstathiou AM (2004) Pt/Mg-Ce-O catalyst for $NO/H_2/O_2$ lean de-NO_x reaction. Environ Chem Lett 2:55–58. https://doi.org/10.1007/s10311-004-0071-x
7. Savva PG, Costa CN (2011) Hydrogen Lean-DeNO_x as an Alternative to the Ammonia and Hydrocarbon Selective Catalytic Reduction (SCR). Catal Rev 53:91–151. https://doi.org/10.1080/01614940.2011.557964
8. Granger P, Dhainaut F, Pietrzik S, Malfoy P, Mamede AS, Leclercq L, Leclercq G (2006) An overview: Comparative kinetic behaviour of Pt, Rh and Pd in the NO + CO and NO + H_2 reactions. Top Catal 39:65–76. https://doi.org/10.1007/s11244-006-0039-0
9. Solomon S, Manning M, Marquis M, Qin D (2007) Climate change 2007 - the physical science basis: Working group I contribution to the fourth assessment report of the IPCC, vol 4. Cambridge university press
10. Macleod N, Lambert RM (2003) Selective NO_x Reduction During the H_2 + NO + O_2 Reaction Under Oxygen-Rich Conditions Over $Pd/V_2O_5/Al_2O_3$: Evidence for In Situ Ammonia Generation. Catal Lett 90:111–115. https://doi.org/10.1023/B:CATL.0000004113.89067.1d
11. Borchers M, Keller K, Lott P, Deutschmann O (2021) Selective Catalytic Reduction of NO_x with H_2 for Cleaning Exhausts of Hydrogen Engines: Impact of H_2O, O_2, and NO/H_2 Ratio. Ind Eng Chem Res 60:6613–6626. https://doi.org/10.1021/acs.iecr.0c05630
12. Hurst NW, Gentry SJ, Jones A, McNicol BD (1982) Temperature Programmed Reduction. Catal Rev 24:233–309. https://doi.org/10.1080/03602458208079654
13. Qi G, Yang R, Rinaldi F (2006) Selective catalytic reduction of nitric oxide with hydrogen over Pd-based catalysts. J Catal 237:381–392. https://doi.org/10.1016/j.jcat.2005.11.025
14. Li X, Zhang X, Xu Y, Liu Y, Wang X (2015) Influence of support properties on H_2 selective catalytic reduction activities and N_2 selectivities of Pt catalysts. Chin J Catal 36:197–203. https://doi.org/10.1016/S1872-2067(14)60197-2
15. Cruciani G (2006) Zeolites upon heating: Factors governing their thermal stability and structural changes. J Phys Chem Solids 67:1973–1994. https://doi.org/10.1016/j.jpcs.2006.05.057
16. Trigueiro F, Monteiro D, Zotin F, Falabella Sousa-Aguiar E (2002) Thermal stability of Y zeolites containing different rare earth cations. J Alloys Compd 344:337–341. https://doi.org/10.1016/S0925-8388(02)00381-X
17. Xin Y, Li Q, Zhang Z (2018) Zeolitic Materials for DeNOx. Selective Catalytic Reduction ChemCatChem 10:29–41. https://doi.org/10.1002/cctc.201700854
18. Wen B (2002) NO reduction with H_2 in the presence of excess O_2 over Pd/MFI catalyst. Fuel 81:1841–1846. https://doi.org/10.1016/S0016-2361(02)00141-2
19. Zheng L, Liu Z, Zhu Q, Li Y, Yu Q, Chen Y, Gong M (2009) $Pt/La\text{-}Ba\text{-}Al_2O_3$/H-ZSM-5 Catalyst for Treating Hydrogen-Powered Vehicle Exhaust. Chin J Catal 30:381–383. https://doi.org/10.1016/S1872-2067(08)60106-0
20. Li L, Wu P, Yu Q, Wu G, Guan N (2010) Low temperature H_2-SCR over platinum catalysts supported on Ti-containing MCM-41. Appl Catal B 94:254–262. https://doi.org/10.1016/j.apcatb.2009.11.016
21. Wang L, Yin C, Yang RT (2016) Selective catalytic reduction of nitric oxide with hydrogen on supported Pd: Enhancement by hydrogen spillover. Appl Catal A 514:35–42. https://doi.org/10.1016/j.apcata.2016.01.013
22. Brunauer S, Emmett PH, Teller E (1938) Adsorption of Gases in Multimolecular Layers. J Am Chem Soc 60:309–319. https://doi.org/10.1021/ja01269a023
23. Groppi G, Ibashi W, Tronconi E, Forzatti P (2001) Structured reactors for kinetic measurements under severe conditions in catalytic combustion over palladium supported systems. Catal Today 69:399–408. https://doi.org/10.1016/S0920-5861(01)00398-4
24. Abazović ND, Comor MI, Dramićanin MD, Jovanović DJ, Ahrenkiel SP, Nedeljković JM (2006) Photoluminescence of

anatase and rutile TiO_2 particles. J Phys Chem B 110:25366–25370. https://doi.org/10.1021/jp064454f
25. Homeyer ST, Sachtler W (1989) Oxidative redispersion of palladium and formation of PdO particles in NaY. Appl Catal 54:189–202. https://doi.org/10.1016/S0166-9834(00)82364-7
26. Duan K, Liu Z, Li J, Yuan L, Hu H, Woo SI (2014) Novel Pd–Au/TiO_2 catalyst for the selective catalytic reduction of NOx by H_2. Catal Commun 57:19–22. https://doi.org/10.1016/j.catcom.2014.07.033
27. Li J, Wu G, Guan N, Li L (2012) NO selective reduction by hydrogen over bimetallic Pd–Ir/TiO_2 catalyst. Catal Commun 24:38–43. https://doi.org/10.1016/j.catcom.2012.03.014
28. Zhang Z, Mestl G, Knözinger H, Sachtler W (1992) Effects of calcination program and rehydration on palladium dispersion in zeolites NaY and 5A. Appl Catal A 89:155–168. https://doi.org/10.1016/0926-860X(92)80230-A
29. Hosseiniamoli H, Bryant G, Kennedy EM, Mathisen K, Nicholson D, Sankar G, Setiawan A, Stockenhuber M (2018) Understanding Structure–Function Relationships in Zeolite-Supported Pd Catalysts for Oxidation of Ventilation Air Methane. ACS Catal 8:5852–5863. https://doi.org/10.1021/acscatal.7b04462
30. Jabłońska M, Król A, Kukulska-Zajac E, Tarach K, Chmielarz L, Góra-Marek K (2014) Zeolite Y modified with palladium as effective catalyst for selective catalytic oxidation of ammonia to nitrogen. J Catal 316:36–46. https://doi.org/10.1016/j.jcat.2014.04.022
31. Li Y, Armor JN (1997) Selective NH_3 oxidation to N_2 in a wet stream. Appl Catal B 13:131–139. https://doi.org/10.1016/S0926-3373(96)00098-7
32. Ueda A, Nakao T, Azuma M, Kobayashi T (1998) Two conversion maxima at 373 and 573K in the reduction of nitrogen monoxide with hydrogen over Pd/TiO_2 catalyst. Catal Today 45:135–138. https://doi.org/10.1016/S0920-5861(98)00261-2
33. Hu Z, Yong X, Li D, Yang RT (2020) Synergism between palladium and nickel on Pd-Ni/TiO_2 for H_2-SCR: A transient DRIFTS study. J Catal 381:204–214. https://doi.org/10.1016/j.jcat.2019.11.006
34. Costa CN, Efstathiou AM (2007) Mechanistic Aspects of the H_2-SCR of NO on a Novel Pt/MgO – CeO_2 Catalyst. J Phys Chem C 111:3010–3020. https://doi.org/10.1021/jp064952o
35. Jones M (1990) Oxidation of hydrogen over supported palladium. J Catal 122:219–229. https://doi.org/10.1016/0021-9517(90)90276-P
36. Hong Z, Wang Z, Chen D, Sun Q, Li X (2018) Hollow ZSM-5 encapsulated Pt nanoparticles for selective catalytic reduction of NO by hydrogen. Appl Surf Sci 440:1037–1046. https://doi.org/10.1016/j.apsusc.2018.01.239
37. Lott P, Wagner U, Koch T, Deutschmann O (2022) Der Wasserstoffmotor – Chancen und Herausforderungen auf dem Weg zu einer dekarbonisierten Mobilität. Chem Ing Tech 94:217–229. https://doi.org/10.1002/cite.202100155
38. Leicht M, Schott FJ, Bruns M, Kureti S (2012) NOx reduction by H_2 on WO_x/ZrO_2-supported Pd catalysts under lean conditions. Appl Catal B 117–118:275–282. https://doi.org/10.1016/j.apcatb.2012.01.023
39. Zhao X, Zhang X, Xu Y, Liu Y, Wang X, Yu Q (2015) The effect of H_2O on the H_2-SCR of NOx over Pt/HZSM-5. J Mol Catal A: Chem 400:147–153. https://doi.org/10.1016/j.molcata.2015.02.013
40. Costilla IO, Sanchez MD, Volpe MA, Gigola CE (2011) Ce effect on the selective catalytic reduction of NO with CH_4 on Pd-mordenite in the presence of O_2 and H_2O. Catal Today 172:84–89. https://doi.org/10.1016/j.cattod.2011.03.025
41. Gutierrez L, Boix A, Decolatti H, Solt H, Lónyi F, Miró E (2012) Further insights on the physico-chemical aspects of PdIn-Hmordenite catalysts for the NOx-SCR with CH_4. Microporous Mesoporous Mater 163:307–320. https://doi.org/10.1016/j.micromeso.2012.07.013
42. Koyano G, Yokoyama S, Misono M (1999) States of Pd in Pd/H–ZSM-5 and Pd/Na–ZSM-5 catalysts and catalytic activity for the reduction of NO by CH_4 in the presence of O_2. Appl Catal A 188:301–312. https://doi.org/10.1016/S0926-860X(99)00222-7
43. Adelman BJ, Sachtler W (1997) The effect of zeolitic protons on NOx reduction over Pd/ZSM-5 catalysts. Appl Catal B 14:1–11. https://doi.org/10.1016/S0926-3373(97)00007-6
44. Barlocher C, McCusker LB (2022) Database of Zeolite Structures. http://www.iza-structure.org/databases/. Accessed 07 Jul 2022
45. Feeley O, Sachtler W (1990) Oxidative redispersion of metals in Y zeolites effect of ammonia on Pd/HY rejuvenation. Appl Catal 67:141–150. https://doi.org/10.1016/S0166-9834(00)84437-1
46. Shibata J, Hashimoto M, Shimizu K, Yoshida H, Hattori T, Satsuma A (2004) Factors Controlling Activity and Selectivity for SCR of NO by Hydrogen over Supported Platinum Catalysts. J Phys Chem B 108:18327–18335. https://doi.org/10.1021/jp046705v
47. Zhang X, Wang X, Zhao X, Xu Y, Gao H, Zhang F (2014) An investigation on N_2O formation route over Pt/HY in H_2-SCR. Chem Eng J 252:288–297. https://doi.org/10.1016/j.cej.2014.05.006
48. Costa CN, Efstathiou AM (2007) Low-temperature H_2-SCR of NO on a novel Pt/MgO-CeO_2 catalyst. Appl Catal B 72:240–252. https://doi.org/10.1016/j.apcatb.2006.11.010